

Surface Modification of Coal-Based Coke Powder with Pitch Powder for Lithium Ion Batteries

Feng Chen, Lulu Ma, Jiangang Ren, Baoxiang Gu, Jiwei Zhang, Pei Ma, Bibo Liu*

School of Resource and Environment, Henan University of Engineering, Zhengzhou 451191, China;

*E-mail: liubb2008@126.com

Received: 3 November 2017 / Accepted: 5 January 2018 / Published: 5 February 2018

As we all know, most of coal-based coke powders are burned as cheap fuel or discarded directly every year, causing serious environmental contamination and enormous waste of resources. Fortunately, previous works have proved that coal-based coke powder is a promising anode material for lithium ion batteries, while the low initial coulombic efficiency and large irreversible capacity of coal-based coke powder limit its large-scale application. In this work, three kinds of surface-modified coal-based coke powders with pitch powder as the anode materials for lithium ion batteries were developed. Results showed that, compared to the samples C_T (prepared with pitch powder pre-coating in toluene solution) and C_A (prepared with pitch powder pre-coating in alcohol solution), the surface modification of coal-based coke powder prepared by mixing the mixture of coke powder and pitch powder (C_M) was found to be the most effective in improving the initial reversible capacity and initial coulombic efficiency of coal-based coke powder. After coating with the pitch-based carbon layer, the initial irreversible capacity of coke powder reduced from 87.5 mAh/g to 65.3 mAh/g, and the initial coulombic efficiency significantly improved from 78.5% to 84.3%. Scanning electron microscopy (SEM) and X-ray diffraction (XRD) were then employed to investigate the samples, the effects of surface modification on the formation of the solid electrolyte interphase (SEI) and the corresponding irreversible capacity losses were discussed. Finally, the influence of the mass contents of pitch powder on the morphology and electrochemical performance of the sample C_M were analyzed.

Keywords: lithium ion batteries; pitch powder; coal-based coke powder; surface modification; electrochemical properties.

1. INTRODUCTION

In modern days, lithium ion batteries have been used widely in most consumer electronic devices, such as mobile phones, laptops, digital cameras, and so on. Since the anode materials dominate the electrochemical properties of the lithium ion batteries, various electrochemically anode materials with high capacity (Si, Sn, Ge, Al, and Sb) have been researched [1]. However, graphite,

with a theoretical capacity of 372 mAh/g, is still the dominating one available in the current market [2, 3].

Coal-based coke powder is the secondary product when coke is crushed for metallurgical and chemical industries, most of which is burned as cheap fuel or discarded directly on account of its high-content impurities and small particle diameters, causing serious environmental contamination and enormous waste of resources [4]. In our previous work, coal-based coke powder has been proved to be a promising anode material for lithium ion batteries because of its low cost, huge availability, eco-friendly, and large reversible capacity. Unfortunately, the initial coulombic efficiency of this coal-based coke powder is only 75.4% [5]. Hence, it is of high importance to develop a process to improve the initial coulombic efficiency of coal-based coke powder as the anode material for lithium ion batteries.

As to commercial graphite anode materials, some researchers have tried to improve their reversible capacities and cycling efficiencies by surface modifications, such as, doping with metals [6-8] or oxides [9, 10], coating with carbonaceous materials [11-15] or polymers [16, 17], and adopting some other modifying methods [18-21]. These results show that surface modification of the natural graphite is an effective method for improving its electrochemical properties for lithium ion batteries.

In this study, a process that with the advantages of simple, effective and environmental friendly was proposed to modify the coal-based coke powder, and the results showed that the surface modification with pitch powder can greatly increase the initial reversible capacity and coulombic efficiency as well as improve the long term cycling performance of coal-based coke powder.

2. EXPERIMENTAL

2.1. Sample preparation

The as-received coal-based coke powder and pitch powder were first crushed and then sieved into granules with an average diameter of around 10 and 4 μm , respectively. The crushed coal-based coke powders were then processed as the following three different pitch powder pre-coating processes, respectively: 1. coal-based coke powder was dispersed in toluene solution that contains pitch powder and then the solvent was evaporated under the temperature of 80 $^{\circ}\text{C}$; 2. coal-based coke powder was dispersed in alcohol solution that contains the pitch powder and then the solvent was evaporated under the temperature of 60 $^{\circ}\text{C}$; 3. coal-based coke powder was mixed with pitch powder by shaking in a bottle for 24 h. The mass ratio of coal-based coke powder and pitch powder was 9:1 in the three processes that mentioned above.

The resulting two kinds of residues (sample 1 and 2) and the mechanical mixture (sample 3) were both heated to 850 $^{\circ}\text{C}$ with a heating ratio of 5 $^{\circ}\text{C}/\text{min}$ and kept for 2 h in nitrogen gas flow, in order to melt the pitch powder to coat the coal-based coke powder more evenly. Finally, the as-obtained three coal-based coke powders with pitch powder pre-coating were treated at 2600 $^{\circ}\text{C}$ for 30 min using a graphite furnace under argon atmosphere, in order to pyrolysis the pitch powder coating into the pitch based-carbon coating and simultaneously increase the degree of graphitization of these

samples. For convenience, the above three kinds of surface-modified coal-based coke powders, which were prepared by the pitch powder pre-coating in toluene solution, in alcohol solution and by mixing the mixture of coke power and pitch powder, were marked as C_T , C_A , and C_M , respectively. Moreover, a contrast sample without surface modification was also prepared under the same conditions described above except using the pitch powder pre-coating process, namely C_C .

2.2. Characterization

The samples were characterized by X-ray diffraction (XRD) with $Cu-K\alpha$ radiation to determine the formed phases. Scanning electron microscopy (SEM) with a working voltage of 15 kV was performed to analyze the surface structure.

2.3. Measurement of electrochemical properties

The working electrodes were composed of coal-based coke powder (with or without surface modification, 80 wt%), acetylene carbon black (10 wt%) to insure electronic conductivity, and polyvinylidene fluoride (PVDF, 10 wt%) as binder. The mixture was dissolved in 1-methyl-2-pyrrolidone (NMP) solution to form homogeneous slurry and then spread onto the copper foils with a scraper blade. Finally, the electrode was dried at 120 °C for 12 h under vacuum. The test electrode was assembled in a 2025 coin-type cell employing lithium foil as the counter electrode, 1 M $LiPF_6$ in ethylene carbonate/dimethyl carbonate (EC/DEC, 1:1, v/v) as the electrolyte, and a polyethylene membrane as the separator. The cell assembly was implemented in a glove box (Super 1220/750, Shanghai Mikrouna Co. Ltd.) filled with Ar gas, in which H_2O and O_2 concentrations were kept below 1 ppm.

The galvanostatic charging-discharging tests were performed on a battery measurement system (LAND CT-2001A, Wuhan Jinnuo Electron Co. Ltd., China) in the potential range of 0.01-2.00 V versus Li/Li^+ at a current density of 0.2 C. The first cycle began with the charge process, corresponding to the insertion of Li^+ into the electrodes.

3. RESULTS AND DISCUSSION

Fig. 1 shows the SEM images of C_C (a and b), C_T (c and d), C_A (e and f), and C_M (g and h), respectively. Compared to the sample C_C without surface modifying, the morphologies of the particles (C_T , C_A , and C_M) after pitch based-carbon coating process did not change appreciably. The products C_T , C_A , and C_M prepared from pitch based-carbon coating can be easily crushed by using fingers to pass through a sieve with an opening of the size of 25 μm . It can be found from Fig. 1 that some razor-sharp edges and chips exist on the edge of C_C , while in the samples C_T , C_A , and C_M , the razor-sharp edges and corners have been rounded generally, and the surfaces of the samples become relatively smooth and tidy. As for the anode materials of lithium ion batteries, the round and neatly morphology are beneficial to the insertion/desertion of lithium ions, and thus noteworthy improving the electrochemical performances [2].

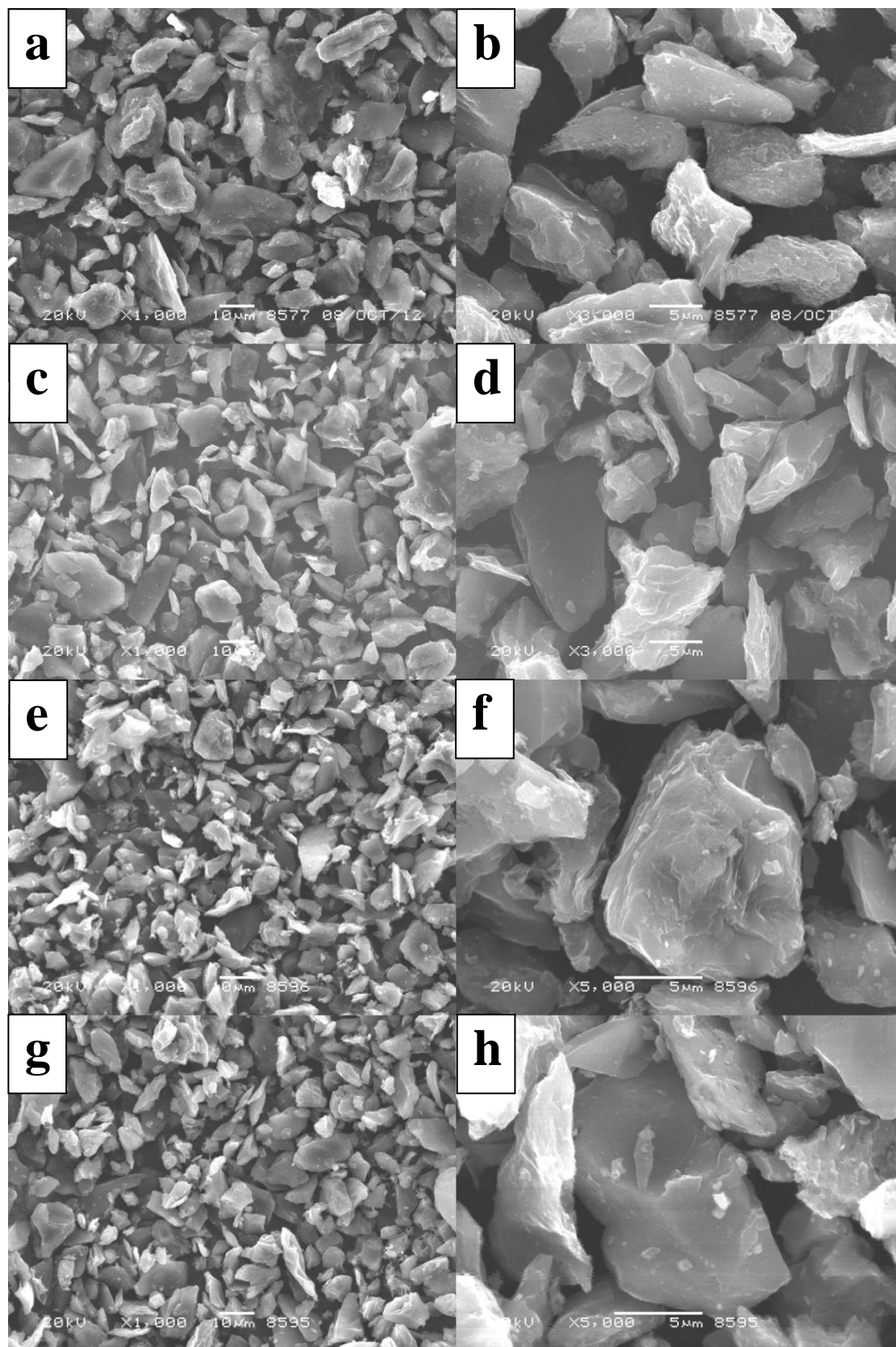


Figure 1. SEM images of C_C (a, b), C_T (c, d), C_A (e, f), and C_M (g, h) at different magnifications.

When comparing the four samples in Fig. 1, the particle size distribution of C_A (Fig. 1e and f) seems to be heterogeneous as there are many small particles, the grain sizes of which are less than 5 μm , and are similar to the particle sizes of pitch powders. These small particles might be the coagulations of residual pitch powders in the coating process. However, the particle sizes of C_T and C_M are almost the same as C_C 's, which have an original average size of 10 μm and almost have no small particles less than 5 μm in diameter. The differences of the average particle size between C_A and C_T/C_M are supposed to be due to the different pitch powder pre-coating processes, which use disparate solvents and mixing approaches. The affection of the morphology variations of C_C , C_A , C_T , and C_M on the electrochemical performances of lithium ion batteries will be discussed in the following section.

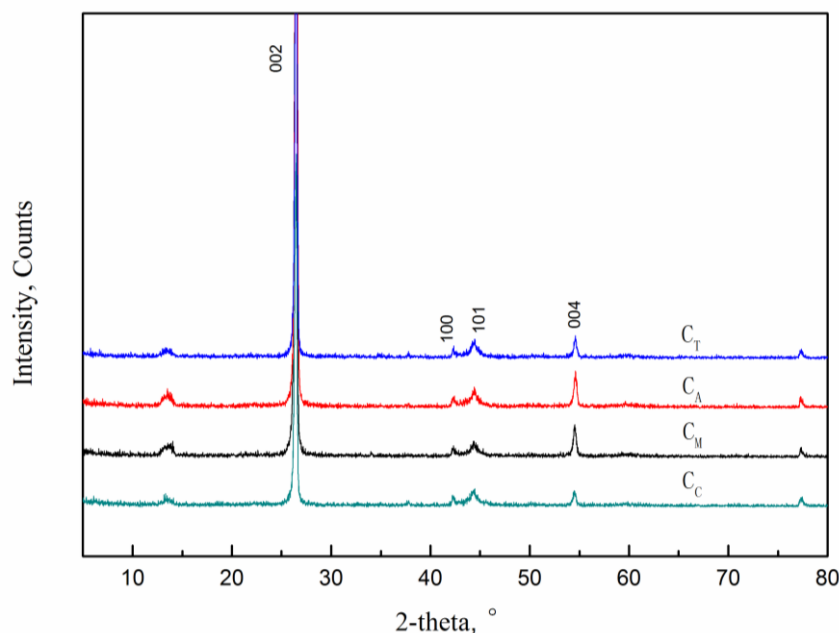


Figure 2. XRD patterns of C_T , C_A , C_M , and C_C from 5° to 80°.

XRD patterns of the four samples C_C , C_T , C_A , and C_M are shown in Fig. 2, respectively. According to these XRD patterns, it can be observed that the four samples display a semblable XRD pattern. The four characteristic peaks located at around 26.3°, 42.4°, 44.3°, and 54.5° can be observed, corresponding to the (002), (100), (101), and (004) planes of hexagonal graphite (JCPDS, No. 41-1487) [22-24], which indicates that the high-temperature heat treatment (2600 °C) is effective for the structural reconstruction of coal-based coke powder, and the carbon-coating process on the coal-based coke powder did not destruct its original structure. However, comparing with the graph from the sample without modifying (C_C), the patterns of the samples with surface modifying (C_T , C_A , and C_M) demonstrate a visible change. The relative peak intensities of these patterns increase lightly, which seems to indicate that the pitch based-carbon coating treatments lead to the increase of crystallinities, this could be because the pitch powder coating can be graphitized more easily than coal-based coke powder. The increase of crystallinities (C_T , C_A , and C_M) implies that slight changes have taken place on the surface morphologies of the samples, i.e. the crystallographic surface layer is formed [25]. This crystallographic film on the coke powder substrate was reportedly available to improve the surface

mechanical performances and resist surface delaminating during the Li⁺ insertion/extraction process, and thus enhancing the cyclic stability of coal-based coke powder [26-28]. Furthermore, among the three modified samples of C_T, C_A, and C_M, the pattern of C_A shows the strongest peak intensity, which could be due to the existence of the coagulations of residual pitch powders, corresponding to the descriptions of Fig.1e and f.

Table 1. The initial discharge and charge test results at 0.2 C.

Sample	Charge capacity (mAh/g)	Discharge capacity (mAh/g)	Irreversible capacity (mAh/g)	Coulombic efficiency (%)
C _C	407.9	320.4	87.5	78.5
C _T	409.6	338.5	71.1	82.6
C _A	369.1	309.5	59.6	83.9
C _M	415.8	350.5	65.3	84.3

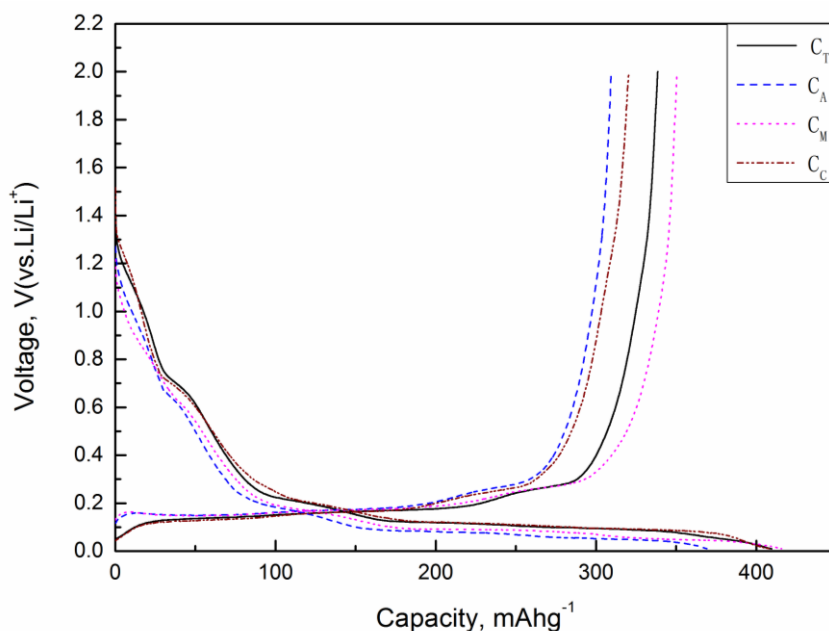


Figure 3. Initial charge and discharge curves of C_T, C_A, C_M, and C_C at 0.2 C.

Table 1 presents the initial charge-discharge capacities, irreversible capacities and coulombic efficiencies of the C_T, C_A, C_M, and C_C samples. In Table 1, the results can be classified into two categories: (I) both the charge capacity and discharge capacity of the sample C_A are lower than those of the sample C_C, this may be related with the unfavorable morphology or the coagulation of particles by residual pitch powders of C_A (Fig.1e and f). However, the samples C_T and C_M have similar charge capacities and discharge capacities to the C_C, and the initial discharge capacities of the three samples

increase from C_C , C_T , to C_M in sequence; (II) the irreversible capacities of the samples C_C , C_T , C_A , and C_M are 87.5, 71.1, 59.6, and 65.3 mAh/g, respectively, which shows that the irreversible capacities of the samples prepared with surface modification are lower than that of sample prepared without modifying. Moreover, in comparison with the initial coulombic efficiency of C_C (78.5%), C_T , C_A , and C_M exhibit higher initial coulombic efficiencies (reaching 82.6%, 83.9%, and 84.3%, respectively). These results are in good consistence with previous studies that the carbon-coating for graphite is an effective way to reduce the initial irreversible capacity and improve the initial coulombic efficiency [26, 27, 29].

Fig. 3 shows the initial charge-discharge curves of C_T , C_A , C_M , and C_C . As can be seen in Fig. 3, the four curves show considerable similarity and significant difference. This behavior may be due to their similar charge-discharge mechanisms and disparate interacting strengths with the electrolyte. The charge profiles of C_T , C_A , C_M , and C_C all exhibit an irreversible voltage plateau at around 0.7 V, which is associated with the decomposition of the electrolyte and the formation of the solid electrolyte interphase (SEI) layer on the interfere between the electrode and the electrolyte [30, 31]. The electrolyte decomposition and the formation of the SEI layer are the reason of irreversible capacities. The passivating SEI layer also can further restrain decomposition of the electrolyte in the following cycles and prohibit the solvent molecules passing through to intercalate into the graphite host, and thus is indispensable for the stability of a graphite electrode [32, 33].

Moreover, the plateau length of C_C (at 0.7 V) is longer than those of C_T , C_A , and C_M , and that of C_M is the shortest and the most non-obvious among the four samples. Therefore, it is evident that C_M is more effective than C_T , C_A , and C_C in suppressing the decomposition of electrolyte. In other words, the pitch based-carbon coating on the coal-based coke powder surface plays a significant role as a barrier for the decomposition of the electrolyte, dramatically decreasing the irreversible capacity. Another long voltage plateau of C_T , C_A , C_M , and C_C appears in the region of 0.2-0.02V, corresponding to the Li^+ intercalation course and a major stage of obtaining Li^+ intercalation capacity. These profiles are characteristic of graphite materials [26]. The shapes of the initial discharge curves of the four samples are analogous, and it is very obvious that the only difference of these discharge profiles is the length of the discharge voltage plateau. The stage of Li de-intercalating of C_T electrode and C_M electrode are similar, which are longer than that of C_C electrode and C_A electrode, i.e. the initial discharge capacities of C_T and C_M are higher than those of C_C and C_A . As for the C_T and C_M electrodes, it can be seen that the initial discharge capacity of C_M is larger than that of C_T , which is in consistent with the results shown in Table 1.

The cycle stabilities of C_T , C_A , C_M , and C_C are examined using long-term cycling tests over 50 cycles at 0.2 C (Fig. 4), which demonstrates that the discharge capacity of sample C_A is slightly unstable with cycling, whereas the other three samples C_T , C_M , and C_C show a relatively good cycling stability. Furthermore, among the three samples C_T , C_M , and C_C , sample C_M shows the largest capacity of about 350 mAh/g during the 50 cycles, which indicates that the C_M electrode has not only high reversible capacity among the four samples but also shows outstanding electrochemical property.

From the above morphologies and electrochemical performances analyses of the four chosen samples (C_T , C_A , C_M , and C_C), it can be inferred that surface modification of coal-based coke powder prepared by mixing the mixture of coke power and pitch powder (C_M) was found to be the most

effective in improving the electrochemical property and reducing the irreversible capacity of coal-based coke powder, what’s more, the modified process is simpler, safer and more environmental friendly than the others.

Furthermore, a comparison of the initial irreversible capacities and coulombic efficiencies between the C_M and other modified graphite-based anodes is presented in Table 2. We can see that the C_M show lower initial irreversible capacity and higher initial coulombic efficiency when compared with previously reported modified graphite-based anodes [23, 34-37], again demonstrating our surface modification process for coal-based coke powder with pith powder is meaningful for enhancing its electrochemical property.

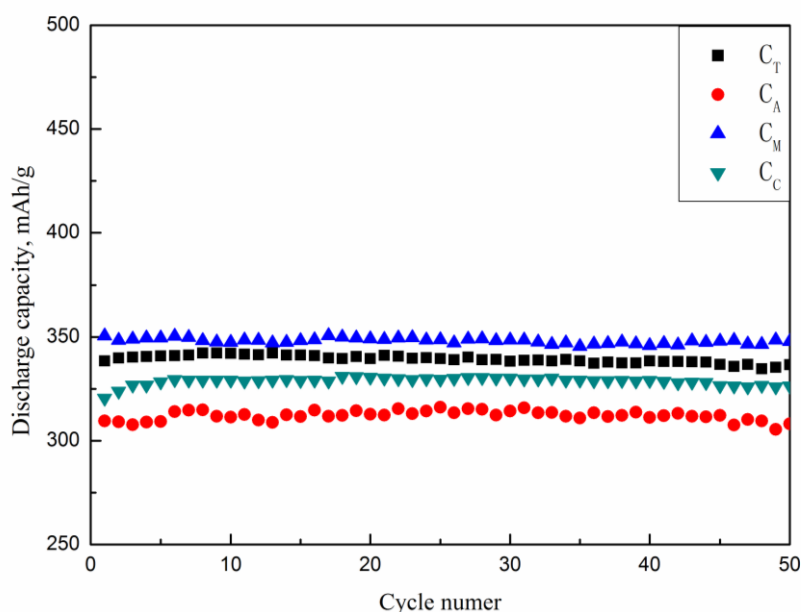


Figure 4. Cycling performances of C_T , C_A , C_M , and C_C over 50 cycles at 0.2 C.

Table 2. Comparison of the initial irreversible capacities and coulombic efficiencies between the C_M and modified graphite-based anodes previously reported.

Sample	Current density	Irreversible capacity (mAh/g)	Coulombic efficiency (%)	Reference
Carbon-coated graphite	0.3 C	84	82	[23]
Activated PVDF/FG	50 mA/g	131.4	78.4	[34]
LiAlO ₂ modified-graphite	0.1 C	~112	~78	[35]
KCl-modified graphite	0.1 C	119	77.2	[36]
PPy-modified graphite	1/15 C	146.5	67.9	[37]
C_M	0.2 C	65.3	84.3	This work

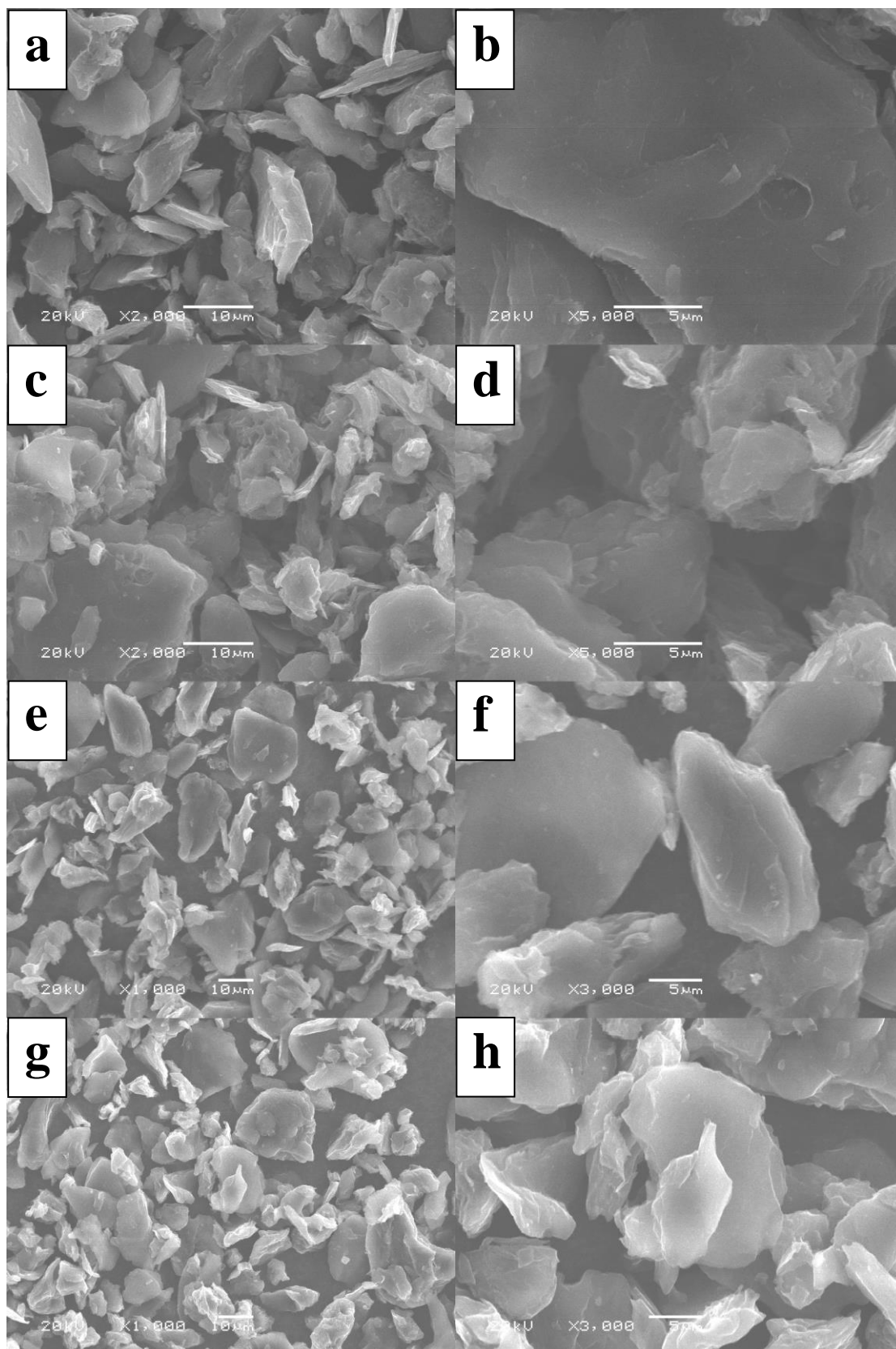


Figure 5. SEM images of C_M-4% (a, b), C_M-10% (c, d), C_M-16% (e, f), and C_M-22% (g, h) at different magnifications.

In order to further investigate the influence of the mass contents of pitch powder on the

morphology and electrochemical performance of the sample C_M , four C_M specimens with different pitch contents (4%, 10%, 16%, and 22%) were also prepared by using the same approach as C_M (described in the above experimental sections), which were denoted as $C_{M-4\%}$, $C_{M-10\%}$, $C_{M-16\%}$, and $C_{M-22\%}$, respectively. Fig. 5 shows the SEM images of $C_{M-4\%}$, $C_{M-10\%}$, $C_{M-16\%}$, and $C_{M-22\%}$. It can be seen that, compared to the sample C_C (Fig. 1a and b), the morphologies of these C_M specimens with different pitch contents did not change obviously, but all exhibiting a smooth and flat surface. The granulometric distributions of $C_{M-4\%}$ and $C_{M-10\%}$ have a uniform distribution, and almost have no small particles less than 5 μm in diameter. However, the granular sizes of the $C_{M-16\%}$ and $C_{M-22\%}$ samples are heterogeneous, and there are many small particles less than 5 μm in diameter. Furthermore, this phenomenon for $C_{M-22\%}$ is more pronounced than $C_{M-16\%}$.

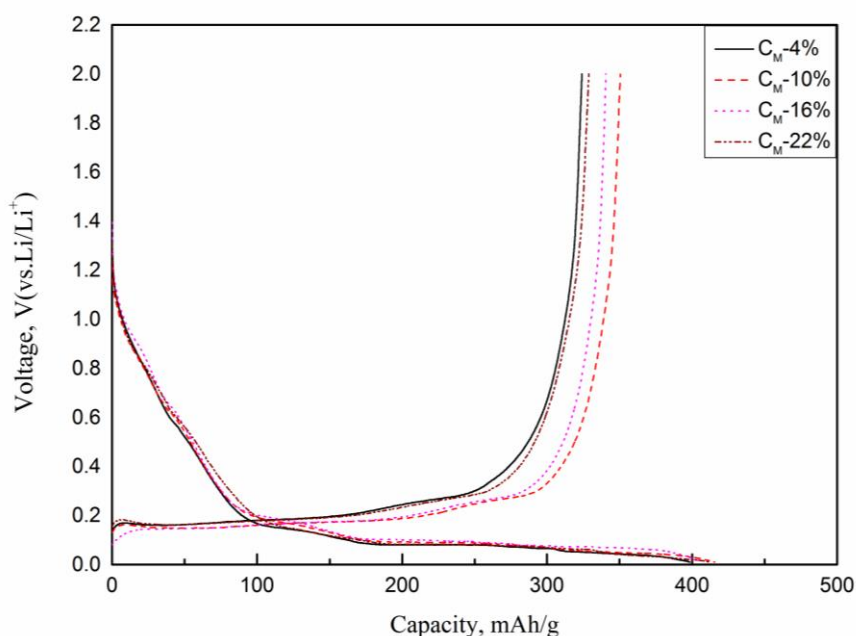


Figure 6. Initial charge and discharge curves of $C_{M-4\%}$, $C_{M-10\%}$, $C_{M-16\%}$, and $C_{M-22\%}$ at 0.2 C.

Table 3. The initial charge/discharge capacities and coulombic efficiencies of $C_{M-4\%}$, $C_{M-10\%}$, $C_{M-16\%}$, and $C_{M-22\%}$ at 0.2 C.

Sample	Content of pitch (wt%)	Charge capacity (mAh/g)	Discharge capacity (mAh/g)	Coulombic efficiency (%)
$C_{M-4\%}$	4	398.5	324.0	81.3
$C_{M-10\%}$	10	415.8	350.5	84.3
$C_{M-16\%}$	16	406.7	340.6	83.8
$C_{M-22\%}$	22	413.1	328.8	79.6

These small particles might be the coagulations of redundant pitch powders during the coating process. Therefore, the above analyses indicate that the mass contents of pitch powders have

a major impact on the morphologies of the C_M specimens, small amounts of pitch powders can't coat the coal-based coke powder effectively, and large amounts of pitch powders would lead to the coagulations of residual pitch.

Fig. 6 shows the initial charge and discharge curves of C_M -4%, C_M -10%, C_M -16%, and C_M -22% at 0.2 C, and the corresponding initial charge/discharge capacities and coulombic efficiencies are summarized in table 3. As shown in Fig. 6, the C_M -4%, C_M -10%, C_M -16%, and C_M -22% all have U-type charge/discharge curves with stable voltage platforms, indicating that various pitch contents in the C_M specimens did not affect their charge and discharge characteristics as the anode materials for lithium ion batteries. Moreover, these charge/discharge curves can be assigned to the characteristic Li^+ insertion/extraction profiles of graphite, and the charge curves corresponding to the insertion of Li^+ into the electrodes [38].

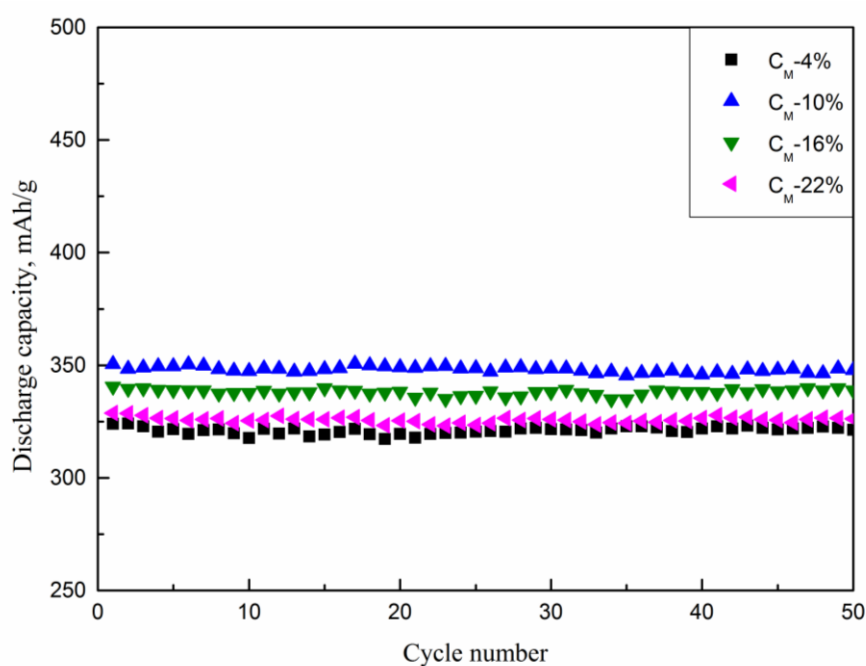


Figure 7. Cycling performances of C_M -4%, C_M -10%, C_M -16%, and C_M -22% over 50 cycles at 0.2 C.

As seen from the table 3, we can see that the initial discharge capacities and coulombic efficiencies of the four C_M samples first increase and then decrease with the increase of the pitch contents, and C_M -10% exhibits the maximum initial discharge capacity and coulombic efficiency of 350.5 mAh/g and 84.3%, respectively. The initial discharge capacity of C_M -4% (324.0 mAh/g) is mostly identical to that of C_M -22% (328.8 mAh/g), but the coulombic efficiency of the former (81.3%) is larger than that of the latter (79.6%). Hence, from the above results, we can conclude that the C_M specimens with appropriate pitch contents would show the best discharge capacity and coulombic efficiency.

The above conjecture was also corroborated by the cycling performances of C_M -4%, C_M -10%, C_M -16%, and C_M -22% at 0.2 C (Fig. 7). These four C_M electrodes all display good cycling performances with negligible capacity fadings over 50 cycles. Moreover, the cycling performances of

$C_{M-10\%}$ and $C_{M-16\%}$ are better than those of $C_{M-4\%}$ and $C_{M-22\%}$. As for the $C_{M-10\%}$ and $C_{M-16\%}$ electrodes, we can see that the cycling performance of $C_{M-10\%}$ is superior to that of $C_{M-16\%}$.

4. CONCLUSIONS

In summary, the surface modifications for coal-based coke powder with three different processes were performed and the effects of these modifications on the electrochemical properties of coke powder were then studied in this work. Compared to the samples C_T (prepared with pitch powder pre-coating in toluene solution) and C_A (prepared with pitch powder pre-coating in alcohol solution), the surface modification of coal-based coke powder prepared by mixing the mixture of coke powder and pitch powder (C_M) was found to be the most effective in improving the initial reversible capacity and initial coulombic efficiency of coal-based coke powder. After coating with the pitch based-carbon layer, the initial irreversible capacity of coke powder reduced from 87.5 mAh/g to 65.3 mAh/g, and the initial coulombic efficiency significantly improved from 78.5% to 84.3%. Moreover, the mass contents of pitch powders have a major impact on the electrochemical performance of the C_M specimens, $C_{M-10\%}$ exhibits the maximum initial discharge capacity of 350.5 mAh/g and the best cycling stability over 50 cycles at 0.2 C. Two reasons for the improvement of electrochemical property by the surface modification with pitch powder have been considered. First, the pitch based-carbon coating in the C_M plays a significant role as a barrier for carbon reacting with electrolyte. Second, the pitch based-carbon coating in the C_M as a crystallographic film on the coke powder substrate improves the surface mechanical properties and resists surface delamination during the charge and discharge process.

CONFLICT OF INTERESTS

The authors declare that there is no conflict of interests regarding the publication of this paper.

ACKNOWLEDGEMENTS

Funding for this work was provided by the National Natural Science Foundation of China (Grant no. 41401549) and the Doctoral Scientific Fund Project of Henan University of Engineering (D2017011).

References

1. W.J. Zhang, *J. Power Sources*, 196 (2011) 13.
2. H.P. Zhao, J.G. Ren, X.M. He, J.J. Li, C.Y. Jiang and C.R. Wan, *Solid State Sci.*, 10 (2008) 612.
3. N.C. Gallego, C.I. Contescu, H.M. Meyer, J.Y. Howe, R.A. Meisner, E.A. Payzant, M.J. Lance, S.Y. Yoon, M. Denlinger and D.L. Wood, *Carbon*, 72 (2014) 393.
4. C.L. Liu, H.M. Luo and G.J. Gou, *Tech. Equip. Environ. Pollut. Control*, 12 (2002) 73.
5. X.Y. Zhou, L.L. Ma, J. Yang, B. Huang, Y.L. Zou, J.J. Tang, J. Xie, S.C. Wang and G.H. Chen, *J. Electroanal. Chem.*, 698 (2013) 39.
6. Y.P. Wu, C.Y. Jiang, C.R. Wan and E. Tsuchida, *Electrochem. Commun.*, 2 (2000) 272.
7. B. Veeraraghavan, A. Durairajan, B. Haran, B. Popov and R. Guidottib, *J. Electrochem. Soc.*, 149 (2002) A675.
8. I.T. Kim, J. Lee, J.C. An, E. Jung, H.K. Lee, M. Morita and J. Shim, *Int. J. Electrochem. Sci.*, 11 (2016) 5807.

9. I.R.M. Kottegoda, Y. Kadoma, H. Ikuta, Y. Uchimoto and M. Wakihara, *Electrochem. Solid-State Lett.*, 5 (2002) A275.
10. Y. Wang, J.Y. Lee and B.H. Chen, *Electrochem. Solid-State Lett.*, 6 (2003) A19.
11. Y.J. Han, J. Kim, J.S. Yeo, J.C. An, I.P. Hong, K. Nakabayashi, J. Miyawaki, J.D. Jung and S.H. Yoon, *Carbon*, 94 (2015) 432.
12. Y.T. Park and K.T. Lee, *Journal of Ceramic Processing Research*, 17 (2016) 1.
13. Y.G. Huang, X.L. Lin, X.H. Zhang, Q.C. Pan, Z.X. Yan, H.Q. Wang, J.J. Chen and Q.Y. Li, *Electrochim. Acta*, 178 (2015) 468.
14. G. Wu, R. Li, Z. Li, J. Liu, Z. Gu and G. Wang, *Electrochim. Acta*, 171 (2015) 156.
15. Y.S. Park, T.W. Lee, M.S. Shin, S.H. Lim and S.M. Lee, *J. Electrochem. Soc.*, 163 (2016) A3078.
16. K.K. Guo, Q.M. Pan and S.B. Fang, *J. Power Sources*, 111 (2002) 350.
17. Y.L. Cao, L.F. Xiao, X.P. Ai and H. Yang, *Electrochem. Solid-State Lett.*, 6 (2003) A30.
18. C. Lee, Y.J. Han, Y.D. Seo, K. Nakabayashi, J. Miyawaki, R. Santamaría, R. Menendez, S.H. Yoon and J. Jang, *Carbon*, 103 (2016) 28.
19. K. Chen, H. Yang, F. Liang and D. Xue, *ACS Appl. Mater. Interfaces*, (2018) DOI: 10.1021/acsami.7b16418.
20. T. Feng, Y. Xu, Z. Zhang, X. Du, X. Sun, L. Xiong, R. Rodriguez and R. Holze, *ACS Appl. Mater. Interfaces*, 8 (2016) 6512.
21. J.S. Yeo, T.H. Park, M.H. Seo, J. Miyawaki, I. Mochida and S.H. Yoon, *Int. J. Electrochem. Sci.*, 8 (2013) 1308.
22. L.Z. Bai, D.L. Zhao, T.M. Zhang, W.G. Xie, J.M. Zhang and Z.M. Shen, *Electrochim. Acta*, 107 (2013) 555.
23. X. Wu, X. Yang, F. Zhang, L. Cai, L. Zhang and Z. Wen, *Ceram. Int.*, 43 (2017) 9458.
24. M. Chen, Z. Wang, A. Wang, W. Li, X. Liu, L. Fu and W. Huang, *J. Mater. Chem. A*, 4 (2016) 9865.
25. J.L. Shui, J. Zhang, C.X. Ding, X. Yang and C.H. Chen, *Mater. Sci. Eng. B*, 128 (2006) 11.
26. H. Wang and M. Yoshio, *J. Power Sources*, 91 (2001) 123.
27. Y.S. Han and J.Y. Lee, *Electrochim. Acta*, 48 (2003) 1073.
28. A. Wang, F. Liu, Z. Wang and X. Liu, *RSC Adv.*, 6 (2016) 104995.
29. H.L. Zhang, F. Li, C. Liu and H.M. Cheng, *J. Phys. Chem. C*, 112 (2008) 7767.
30. X. Zhou, F. Chen, T. Bai, B. Long, Q. Liao, Y. Ren and J. Yang, *Green Chem.*, 18 (2016) 2078.
31. Q. Shi, W. Liu, Q. Qu, T. Gao, Y. Wang, G. Liu, V.S. Battaglia and H. Zheng, *Carbon*, 111 (2017) 291.
32. H. Li and H. Zhou, *Chem. Commun.*, 48 (2012) 1201.
33. H. Zhao, J. Ren, X. He, J. Li, C. Jiang and C. Wan, *Electrochim. Acta*, 52 (2007) 6006.
34. J. Chen, G. Zou, Y. Zhang, W. Song, H. Hou, Z. Huang, H. Liao, S. Li and X. Ji, *Electrochim. Acta*, 196 (2016) 405.
35. Y. Wu, Y.F. Li, L.Y. Wang, Y.J. Bai, Z.Y. Zhao, L.W. Yin and H. Li, *Electrochim. Acta*, 235 (2017) 463.
36. Y. Wu, L.Y. Wang, Y.F. Li, Z.Y. Zhao, L.W. Yin, H. Li and Y.J. Bai, *J. Phys. Chem. C*, 121 (2017) 13052.
37. B. Veeraraghavan, J. Paul, B. Haran and B. Popov, *J. Power Sources*, 109 (2002) 377.
38. H.P.T.S. Hewathilake, N. Karunarathne, A. Wijayasinghe, N.W.B. Balasooriya and A.K. Arof, *Ionics*, 23 (2017) 1417.